

Enhanced diamagnetism in intense magnetic field in the pseudogap state of the cuprate $\text{Bi}_2\text{Sr}_2\text{CaCu}_2\text{O}_{8+\delta}$

Yayu Wang¹, Lu Li¹, M. J. Naughton², G. D. Gu³, S. Uchida⁴, N. P. Ong¹

¹*Department of Physics, Princeton University, New Jersey 08544, U.S.A.*

²*Department of Physics, Boston College, Chestnut Hill, Massachusetts 02467, U.S.A.*

³*Department of Physics, Brookhaven National Laboratory, Upton, N.Y. 11973.*

⁴*School of Frontier Science, University of Tokyo, Tokyo 113-8656, Japan.*

(Dated: December 2, 2024)

In high-temperature superconductors, a strongly debated issue is whether the superconducting state is destroyed by spontaneous creation of vortices which disorder the phase of the macroscopic wave function. This scenario is supported by Nernst experiments but lacks confirmation from other experiments, notably magnetization. Using high-resolution torque magnetometry, we uncover a magnetization signal above the transition that survives to a field of 32 Tesla and scales like the Nernst signal. The evidence, together with the unusual behavior of the the upper critical field provide strong evidence for the vortex scenario.

In bulk superconductors, the transition out of the superfluid state involves the vanishing of the macroscopic wave function $\hat{\Psi}$, but in hole-doped cuprates there is growing evidence that the transition is caused by the proliferation of vortices which destroy long-range phase coherence. The detection of a large Nernst signal e_N and kinetic inductance above the critical transition temperature T_c has provided evidence for the vortex scenario [1, 2, 3, 4, 5, 6]. However, because the thermodynamic evidence – notably magnetization – is unsettled, lingering doubt about the vortex-scenario interpretation of e_N persists. Using high-field, high-resolution torque magnetometry on $\text{Bi}_2\text{Sr}_2\text{CaCu}_2\text{O}_{8+\delta}$ (Bi 2212), we show the existence of an enhanced diamagnetism above T_c that closely matches the Nernst signal as a function of both field H and temperature T . In addition to establishing the unusual nature of the transition and its diamagnetic state above T_c , the high-field magnetization provides an improved estimate of the upper critical field $H_{c2}(T)$ and clarifies its unusual behavior near T_c .

In the superconducting state, the condensate wave function $\hat{\Psi} = |\hat{\Psi}|e^{i\theta}$ strives to maintain rigid uniformity in its phase θ throughout the sample. This long-range phase coherence, essential for superfluidity, is easily destroyed by mobile vortices, which the Nernst-effect experiment has observed in cuprates. However, despite the loss of phase coherence, we should expect local supercurrents and a magnetization M proportional to $|\hat{\Psi}|^2$ to be observable in the vortex liquid [7]. Hence magnetization evidence is essential for the vortex scenario.

It turns out that resolving this issue demands measurements of the magnetization M to much higher fields and resolution. To achieve these conditions, we used a sensitive torque magnetometer [8] in which the crystal is glued to the tip of a micro-machined single-crystal Si cantilever with its c -axis at a tilt-angle $\varphi_0 \sim 15^\circ$ to \mathbf{H} (Fig. 1, inset). The torque $\boldsymbol{\tau} = \mathbf{m} \times \mathbf{B}$ leads to a flexing of the cantilever which is detected capacitively, where \mathbf{m} is the sample's magnetic moment and $\mathbf{B} = \mu_0\mathbf{H}$ with μ_0 the vacuum permeability. In all measurements, the maximum deflection of the cantilever is $< 0.15^\circ$, or 100 times

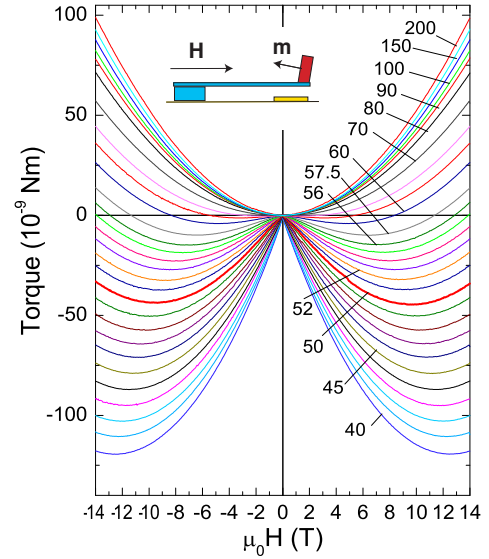


FIG. 1: The measured torque τ vs. H at selected T in underdoped Bi 2212. Curves from 130-200 K are parabolic consistent with $M_{para} = \chi_p H$, with $\chi_p > 0$. Below 130 K, a diamagnetic contribution M grows rapidly. The bold curve indicates $T_c = 50$ K. At some T , measurements were extended to 32 T. The inset shows the Si cantilever and the magnetic moment \mathbf{m} of the crystal.

smaller than φ_0 . We can resolve $m \sim 5 \times 10^{-9}$ emu at 10 T. Measurements in a SQUID magnetometer (with resolution $\sim 10^{-6}$ emu) were performed to complement the torque results. We note that torque magnetometry has been done before on cuprates [8, 9, 10]. However, the results here in intense field, especially the scaling with the Nernst signal, point us to a set of conclusions very different from earlier studies.

The torque curves measured in an underdoped (UD) Bi 2212 crystal, with $T_c = 50$ K, are shown in Fig. 1. From 130 to 200 K, τ varies as H^2 , reflecting a paramagnetic

susceptibility χ that is only weakly T dependent. Below 120 K, a significant diamagnetic contribution becomes apparent. With decreasing T , the curves develop double minima which deepen rapidly. This reflects the growth of in-plane screening currents that eventually pull the torque to negative values. Similar curves were obtained in an optimally-doped (OP) crystal with $T_c = 87.5$ K, as well as an overdoped (OD) crystal doped with Pb with $T_c = 79$ K. All curves of M reported here are *fully reversible* in H and T . In the OP sample, slight hysteresis below ~ 2 T becomes observable for $T < 35$ K. The Nernst signal e_N was measured in the same crystals (details on the Nernst experiment are in Ref. [2, 3, 4]).

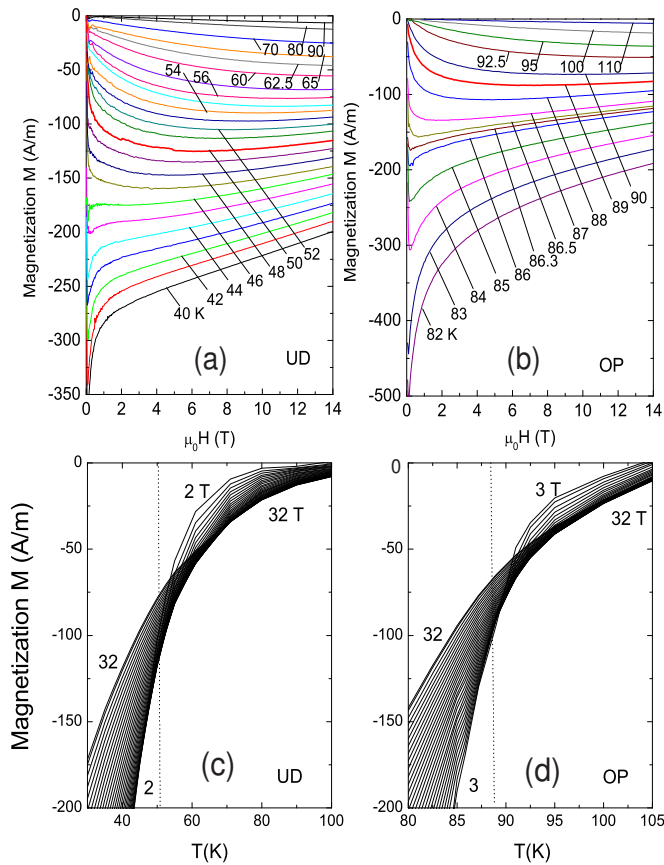


FIG. 2: Curves of magnetization $M = M_{tot} - \chi_p H$ plotted vs. H at selected T in the (Panels a and b), and plotted vs. T in (c and d) for the UD and OP samples as indicated. In (a) and (b), the bold curve is taken at T_c . In Panels (c) and (d), the T dependence of M is plotted at fixed H in the UD and OP sample, respectively [H decreases, in steps of 1 Tesla, from 32 T to 2 T in (a) and 3 T in (b)]. The curves emphasize the smooth variation of $M(H, T)$ near T_c . Broken lines indicate T_c .

The total magnetization is related to the torque by $M_{tot}(T, H) = \tau/BV \sin \varphi_0$ with V the crystal volume. The curves in Fig. 1 show that M_{tot} is the sum of a paramagnetic term $M_{para} = \chi_p H$, and a strongly T dependent diamagnetic term $M(T, H)$, which is our main

interest. The weak T dependence of the paramagnetic χ_p allows $M(T, H)$ to be extracted cleanly.

Figure 2 compares the M vs. H curves in the UD and OP samples. In the UD sample [Panel (a)], a large diamagnetic signal appears at ~ 120 K and grows over an extended interval (70 K) as T approaches T_c (bold curve). As T falls below T_c , rapid changes caused by the growth of the Meissner signal become apparent in low H . The curves in Fig. 2b behave in a similar way except that the interval above T_c with enhanced diamagnetism is narrower (30 K). The T dependences of the magnetization in fixed H are displayed in Figs. 2c and 2d for fields up to 32 T. Previously, low-field experiments [11, 12] seemed to show that all curves of M vs. T intersect at a single ‘crossing temperature’, but measurements to higher fields [8] have shown that the intersections are actually spread over a broad range of T , which we confirm here. For our purpose, two features in Fig. 2 are rather more significant, namely the robustness of the signal above T_c up to 32 T and the absence of an abrupt change in the slope dM/dT across T_c .

At first glance, the curves in Fig. 2 recall the well-known ‘fluctuation diamagnetism’ studied in low- T_c type II superconductors which are produced by evanescent superfluid droplets caused by fluctuations of the amplitude $|\hat{\Psi}|$ [13, 14, 15]. These amplitude (or Gaussian) fluctuations are *extremely sensitive to field*, becoming unresolved once H exceeds a few 100 Oe (the H dependences in Nb, In and Pb and alloys are shown in Fig. 13 of Ref. [14]). Weak diamagnetism above T_c in cuprates has been observed previously [8, 12, 16, 17, 18], but was mostly analyzed as amplitude fluctuations, with scant attention paid to the effect of a strong H (with Ref. [17] as an exception).

Our experiment shows that the diamagnetism in Bi 2212 is qualitatively different from low- T_c superconductors. The evidence are of 3 types. First, we focus on $T > T_c$. As apparent in Fig. 2, in a field of 32 T, M survives as a long tail over a 70-K interval (30-K interval) above T_c in the UD (OP) sample. This robustness in intense fields – incompatible with amplitude fluctuations – sharply distinguishes the cuprate signal from that in low- T_c superconductors. The rapid suppression by H of Gaussian fluctuations in the latter stems from the concomitant decrease of the amplitude $|\hat{\Psi}|$ and $H_{c2}(T)$ towards zero at T_c . However, as noted in Fig. 2, the curves of M vs. T show no sign of a change-in-slope as a function of either H or T , suggestive of a vanishing $|\hat{\Psi}|$ ($H_{c2}(T)$ is discussed below).

Secondly, we show that the diamagnetic signal above T_c is closely related to the Nernst signal. In Figs. 3a and 3b, we plot the T dependence of e_N and M (both at 14 T) in the UD and OP samples, respectively (the Meissner signals measured in 10 Oe are shown as dashed curves). Remarkably, M (solid circles) tracks e_N (open) over a broad interval of temperature before diverging near T_c . Below T_c , M rises steeply whereas e_N attains a broad peak before decreasing towards zero (its value in the vor-

tex solid phase). The 2 signals M and e_N share the same onset temperatures T_{onset} .

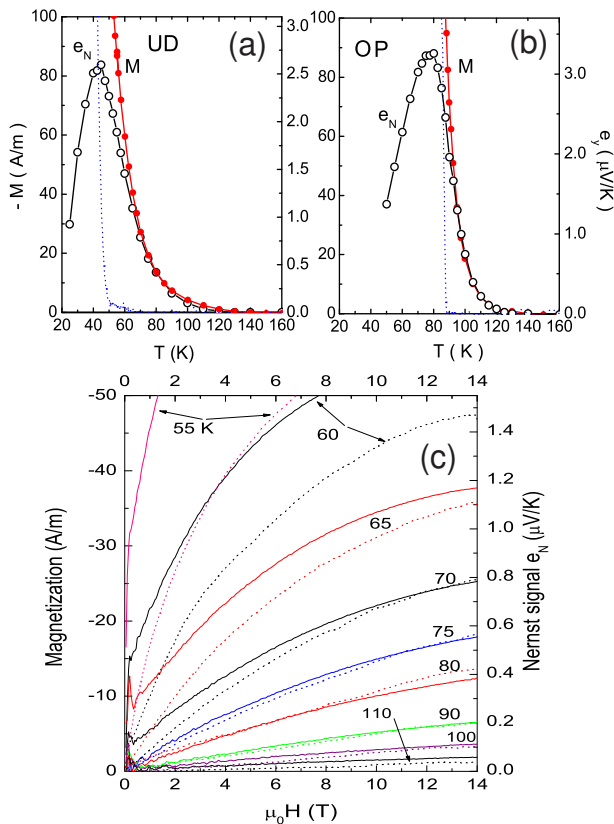


FIG. 3: Comparison of M and the vortex-Nernst signal e_N measured at 14 T in the UD (Panel a) and OP (b) Bi 2212, and comparison of their field profiles in UD Bi 2212 (Panel c). In Panels (a) and (b), M and e_N track each other at high T . Below T_c , M increases rapidly while e_N attains a peak before falling towards zero in the vortex-solid phase. The dashed curves show M measured in $H = 10$ Oe in a SQUID magnetometer. Panel (c) shows that curves of M vs. H (solid curves) match those of e_N vs. H (dashed curves) in the UD sample above T_c (the scale factor between M and e_N is the same as in Panel a). The observed Nernst signal is the sum of the vortex contribution and a quasiparticle (qp) term $e_N^{obs} = e_N + e_N^{qp}$. The negative qp term e_N^{qp} has been subtracted from the observed Nernst signal.

In both samples, the direct proportionality between M and e_N above T_c also holds as H is varied. We compare their respective field profiles in the UD sample in Fig. 3c. Over the interval 70-120 K, we find that the M vs. H curves (solid) can be overlaid on the e_N vs. H curves (dashed) with the same scaling factor as in Fig. 3a. In terms of the resistivity ρ and α_{yx} , we have $e_N = \rho \alpha_{yx}$ [the quantity α_{yx} relates the transverse charge current J_y to the gradient, viz. $J_y = \alpha_{yx}(-\partial_x T)$]. The scaling relationship is then $\alpha_{yx} = -\beta M$ for $T > T_c$. The linear relationship between M and α_{yx} close to H_{c2} was calculated by Caroli and Maki [19], and later corrected for the magnetization current [20, 21]. The plots in Fig. 3 confirm that, above T_c , the growth of e_N is accompanied by

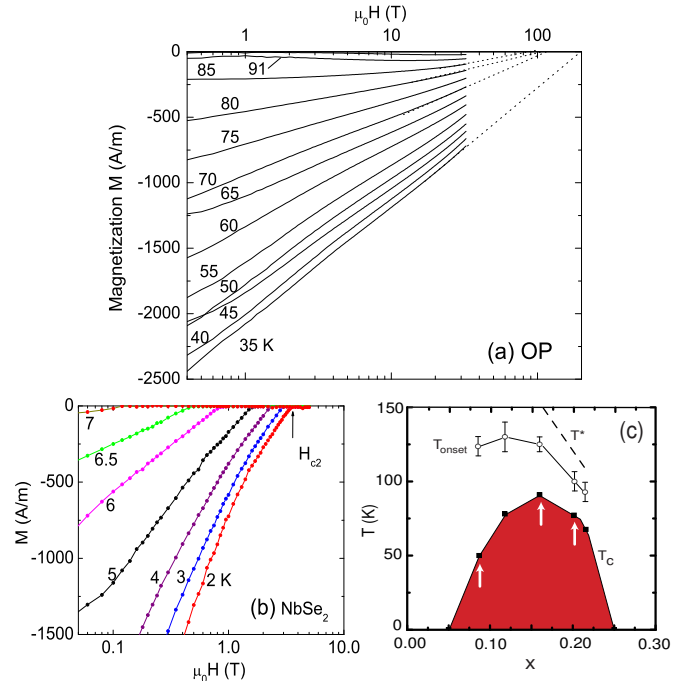


FIG. 4: Plot of the field dependence of M in OP Bi 2212 (Panel a) and in NbSe₂ (b) and the phase diagram of Bi 2212 (Panel c). In Panel a, the measured M extends from 0.4 to 32 T at temperatures 35 K to 91 K. Nominally, $|M|$ decreases linearly with $\log H$. The $H_{c2}(T)$ values estimated by extrapolation (broken lines) remain at above 90 T as $T \rightarrow T_c$ (87.5 K). In Panel b, the measured M also shows a nominally linear dependence on $\log H$. However, in contrast with (a), $H_{c2}(T)$ decreases from 3.6 T to 0.12 T as T rises from 2 to 7 K. In Panel c, T_{onset} of both M and e_N is plotted vs. x (hole content) together with T_c and T^* . Arrows indicate the 3 samples studied by torque magnetometry.

an increase in the strength of the screening diamagnetic current as required by the vortex scenario.

Lastly, we describe the behavior of $H_{c2}(T)$ inferred from the curves at $T < T_c$ (Fig. 4a). In type II superconductors, M decreases linearly to zero as $M \sim -[H_{c2}(T) - H]$ in mean-field theory [7]. It is generally agreed that the field at which $M \rightarrow 0$ provides the best way to determine $H_{c2}(T)$. In Fig. 4b we plot M in NbSe₂ (measured by SQUID magnetometry) against $\log H$. The values of $H_{c2}(T)$, defined by the end points of M , approach zero linearly in the reduced temperature $t = 1 - T/T_c$ as $T \rightarrow T_c^-$ (to logarithmic accuracy $H_{c2}(T)$ may be estimated by linear extrapolation of $-M \sim \log H$ to the H -axis). As noted, the vanishing of $H_{c2}(T)$ causes the amplitude fluctuations to be sensitive to field.

The curves of $H_{c2}(T)$ in Bi 2212 behave in a qualitatively different way. Figure 4a plots the curves of M vs. $\log H$ in the OP sample from 0.4 T to 32 T at temperatures 35 to 91 K. At each T , the decrease in M is nominally linear in $\log H$, but M clearly retains signifi-

cant strength at 32 T. Instead of going to zero, $H_{c2}(T)$ remains high above 32 T as $T \rightarrow T_c$, consistent with the H_{c2} behavior inferred from e_N [3, 4]. The contrast with low- T_c superconductors is quite striking (similar conclusions are obtained in the UD sample).

If we assume that M remains nominally linear in $\log H$ above 32 T (as suggested by the curves for NbSe₂), we may estimate H_{c2} with logarithmic accuracy. The broken lines suggest that H_{c2} decreases from 200 T to ~ 90 T between 35 K and 85 K. The value at 85 K is nominally similar to the estimate from e_N in Ref. [4].

Taken together, the evidence suggest that H_{c2} remains at ~ 90 T as T crosses T_c . Hence, above the melting line $H_m(T)$, the amplitude $|\hat{\Psi}|$ is finite beyond our highest field 32 T, but the phase θ is strongly disordered. The vortex-liquid state starts at $H_m(T)$ (for $T < T_c$) and continues smoothly to T_{onset} . The present results establish an essential link between the magnetization and the Nernst experiments above T_c . In equilibrium in H , local screening supercurrents in the vortex liquid are observed as a robust diamagnetic signal, while in an applied gradient $-\nabla T$ the flow of vortices leads to a large Nernst

signal proportional to M . In zero field, the collapse of the Meissner effect at T_c arises from the spontaneous creation of vortices which destroy long-range phase coherence [22].

As shown in Panel (c), T_{onset} lies significantly below the pseudogap temperature T^* determined from photoemission [23, 24] and nuclear magnetic resonance (NMR) relaxation experiments [25, 26, 27]. The extension of the vortex-liquid state above T_c in Fig. 3c implies a close relationship between the pseudogap state and d -wave superconductivity. It suggests that Cooper pairing with a large binding energy already exists over some fraction of the pseudogap state, but phase coherence develops gradually on cooling. However, we remark that the enhanced M and e_N above T_c depend crucially on the presence of the pseudogap which appears only in the hole-doped cuprates. If the pseudogap is absent – as in the electron-doped Nd_{2-x}Ce_xCuO₄ – the vortex-Nernst signal above T_c is absent [4]. Hence the origin of the enhanced M and e_N is deeply entwined with the physics of spin-singlet formation and the spin-gap [25, 26] that opens at T^* higher than T_{onset} .

-
- [1] Z. A. Xu, N. P. Ong, Y. Wang, T. Kakeshita, S. Uchida, Nature **406**, 486 (2000).
- [2] Yayu Wang *et al.*, Phys. Rev. B **64**, 224519 (2001).
- [3] Yayu Wang *et al.*, Phys. Rev. Lett. **88**, 257003 (2002).
- [4] Yayu Wang *et al.*, Science, **299**, 86 (2003).
- [5] N. P. Ong and Yayu Wang, Physica C **408**, 11-14 (2004).
- [6] J. Corson, R. Mallozzi, J. Orenstein, J. N. Eckstein, and I. Bozovic, Nature **398**, 221 (1999).
- [7] *Superconductivity of Metals and Alloys*, P. G. deGennes (Addison-Wesley, 1989), p. 201.
- [8] M. J. Naughton, Phys. Rev. B **61**, 1605 (2000).
- [9] C. Bergemann *et al.*, Phys. Rev. B **57**, 14387 (1998).
- [10] J. Hofer *et al.*, Phys. Rev. B **62**, 631 (2000).
- [11] P. Kes *et al.*, Phys. Rev. Lett. **67**, 2383 (1991).
- [12] U. Welp *et al.*, Phys. Rev. Lett. **67**, 3180 (1991).
- [13] R. Prange, Phys. Rev. **1**, 2349 (1970).
- [14] J. P. Gollub, M. R. Beasley, R. Callarotti, and M. Tinkham, Phys. Rev. B **7**, 3039 (1973).
- [15] P. A. Lee and M. G. Payne, Phys. Rev. Lett. **26**, 1537 (1971).
- [16] Q. Li *et al.*, Phys. Rev. B **48**, 9877 (1993).
- [17] V. G. Kogan *et al.*, Phys. Rev. Lett. **70**, 1870 (1993).
- [18] C. Carballera, J. Mosqueira, R. Revcolevschi, and F. Vidal, Phys. Rev. Lett. **84**, 3517 (2000).
- [19] C. Caroli, and K. Maki, Phys. Rev. **164**, 591 (1967).
- [20] C. R. Hu, Phys. Rev. B **13**, 4780 (1976).
- [21] I. Ussishkin and S. L. Sondhi, cond-mat/0406347.
- [22] V. J. Emery and S. A. Kivelson, Nature **374**, 434 (1995).
- [23] Ding H. *et al.*, Nature **382**, 51 (1996)
- [24] Loeser A.G. *et al.*, Science **273**, 325 (1996)
- [25] H. Alloul *et al.*, Phys. Rev. Lett. **67**, 3140 (1991)
- [26] M. Takigawa *et al.*, Phys. Rev. B **43**, 247 (1991)
- [27] Nakano T. *et al.*, Phys. Rev. B **49**, 16000 (1994)
- [28] We thank P. A. Lee, S. Sondhi and I. Ussishkin for helpful comments. High-field measurements were performed at the National High Magnetic Field Laboratory, Tallahassee, which is supported by the U.S. National Science Foundation (NSF) and the State of Florida. This research is supported by NSF Grant DMR 0213706. GDG was supported by the DOE under contract No. DE-AC02-98CH10886.